ELSEVIER
Journal of Nuclear Materials 283–287 (2000) 423–427
journal of nuclear materials
www.elsevier.nl/locate/jnucmat

# The contribution of various defects to irradiation-induced hardening in an austenitic model alloy

M. Ando [a,*], Y. Katoh [a], H. Tanigawa [b], A. Kohyama [a], T. Iwai [c]

[a] Institute of Advanced Energy, Kyoto University, Gokasho, Uji, Kyoto 611-0011, Japan
[b] Japan Atomic Energy Research Institute, Tokai 319-1195, Japan
[c] Research Center of Nuclear Science and Technology, University of Tokyo, Tokai-mura, Naka-gun, Ibaraki 319-11, Japan

**Abstract**

The combination of charged particle irradiation using MeV energy range accelerators and an ultra-low load indentation is a potential technique to study the mechanical property changes of fusion structural materials due to high-energy neutron irradiation. This work was intended to examine the contribution of various defects to irradiation-induced hardening in an Fe–15Cr–20Ni model alloy by means of single/dual-beam ion irradiation and a micro-indentation. In single/dual ion-irradiated specimens, a significant reduction in Frank loop number density was observed in a region where indentation-induced dislocations evolved. It was observed that only Frank loops with diameters of about 20 nm partially survived in the plastically deformed region. In the dual ion-irradiated specimens, cavities shear-deformed along the mass-flow directions were observed in the region beneath the indent. It was concluded through the indentation hardness determination and post-irradiation indentation micro-structural examination that small Frank loops cause hardening to a larger extent than expected from their actual sizes and induce plastic instability by annihilating by interactions with moving dislocations, while clean cavities produced by ion irradiation are not strong deformation barriers as estimated from neutron data. 

## 1. Introduction

Changes in mechanical properties produced by high-energy neutron irradiation can strongly affect the behavior of materials. Particularly, hardening and ductility degradation are among the crucial engineering issues for both fusion structural and functional components. The ductility degradation and accompanying matrix hardening observed in austenitic stainless steels, which are neutron irradiated at about 473–673 K, are phenomenologically understood to a certain extent [1], but the underlying mechanism of irradiation-induced hardening has not been clearly explained.

Single/dual-beam irradiation using MeV energy range accelerators, with simultaneous irradiation with metallic ions and helium ions, is an effective experimental technique to study irradiation-induced phenomena in fusion materials, mainly because irradiation conditions such as displacement damage rate, He/dpa ratio and irradiation temperature can accurately be controlled. However, such a technique is not generally recognized to be suitable for studies on mechanical properties because of the limited penetration depth of the ions in that energy range, except when combined with the use of ultra-low load indentation technique or micro-indentation technique.

Micro-indentation measurement on ion-irradiated materials was successfully performed by Zinkle et al. [2] for relatively high-energy ions and more recently applied to various materials including light water reactor pressure vessel steels [3] and reduced-activation ferritic steels [4]. A previous paper covered the development of the experimental technique and some initial results conducted on a model austenitic alloy [5]. The present work is intended to examine the irradiation-produced defects (e.g., Frank loop, stacking fault tetrahedron (SFT) and cavity), and their interaction with indentation-induced dislocation motion in an austenitic model alloy, and to evaluate the contribution of various defects to

* Corresponding author. Tel.: +81-774 38 3466; fax: +81-774 38 3467.
*E-mail address:* andy@iae.kyoto-u.ac.jp (M. Ando).


PII: S0022-3115(00)00366-4

irradiation-induced hardening in single/dual ion-irradiated specimens.

## 2. Experimental procedure

The material used in this study was a polycrystalline Fe–15Cr–20Ni austenitic model ternary alloy in a solution-annealed condition. The detailed description of the material has been published elsewhere [6]. A sheet of the model alloy was cut into specimens of the small coupon type using a high-speed precision cutting machine. The size of the specimens was $2\times3\times0.2$ mm$^3$ and one of the $3\times0.2$ mm$^2$ sides was irradiated after a diamond-polishing followed by an electrolytic surface finishing.

The ion-beam irradiation experiment was carried out at the high-fluence irradiation facility, University of Tokyo (HIT Facility) [7]. The atomic displacement damage was introduced by 4 MeV $Ni^{3+}$ ions accelerated with a Tandetron tandem accelerator operating at 1 MV. The irradiation temperature, displacement dose range and displacement rate were 723–873 K, 4–25 displacements per atom (dpa) and $1\times10^{-3}$ dpa/s, respectively. In the dual ion-irradiation experiment, 1 MeV $He^{+}$ generated by a Van de Graaff accelerator was bombarded through a rotating nickel foil energy degrader operated so that the He/dpa ratio might be constant at 10 appm He/dpa in a range 400–700 nm from the incident surface. The nominal displacement dose and rate are the average over the 1 μm thick layer at the irradiated surface, as calculated by the TRIM-92 code [8] assuming 40 eV of average displacement threshold energy.

The irradiated specimens were then indentation-tested at a load range 2.34–9.8 mN using an Akashi MZT-3 instrumented micro-indentation testing system. The direction of indentation was chosen to be in parallel to the ion beam axis, i.e., normal to the irradiated surface. The shape of the indenter tip was triangular pyramidal with the semi-apex angle of 68°. The unirradiated and irradiated specimens' regions right beneath the indents were made into thin films, with a JEOL/Micrion JFIB-2100 focused ion beam (FIB) processing system. The foils were made so that they include the indentation axis. Fig. 1 illustrates the procedure of cross-sectional thin foil processing for transmission electron microscope (TEM) examination. The ion beam used in this process was gallium ion accelerated at 30 kV. The micro-structural examination was carried out using a JEOL JEM-2010 EX TEM operating at 200 kV.

## 3. Results and discussions

### 3.1. Micro-indentation hardness

Table 1 shows results of micro-indentation hardness determination in unirradiated and single/dual-beam irradiated specimens. A detailed description of a method of micro-indentation hardness profiling has been published elsewhere [4]. The micro-hardness of unirradiated specimens was 1.25 GPa. This micro-hardness corresponds to a Vickers hardness number of about 113, which agrees well with the typical number of austenitic model alloy in a solution-annealed condition. The average micro-hardness of a specimen irradiated with single ion at 723 K was 2.4 GPa, where the major micro-structural contributors to the hardening were Frank loops of interstitial type and network dislocations. On the other hand, dual ion irradiation at 873 K that produced cavities and network dislocations yielded a hardness of 1.6 GPa.

### 3.2. Cross-sectional TEM observation

Fig. 2(a) shows a cross-sectional TEM dark field image in a region well apart from the indent in the single ion-irradiated specimen (723 K, 4 dpa). The zone-axis is

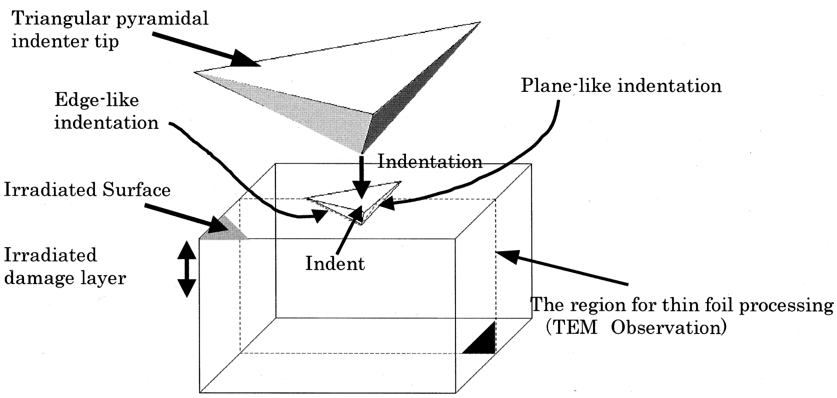


Fig. 1. Illustration of the indent following micro-indentation and the region of TEM observation for the indent.

Table 1
The averaged micro-indentation hardness of single/dual ion-irradiated specimens in the Fe–15Cr–20Ni austenitic model alloy

| | Unirradiated | Single ion-irradiated | Dual ion-irradiated |
|---|---|---|---|
| Micro-indentation hardness | 1.25 GPa | 2.4 GPa | 1.6 GPa |

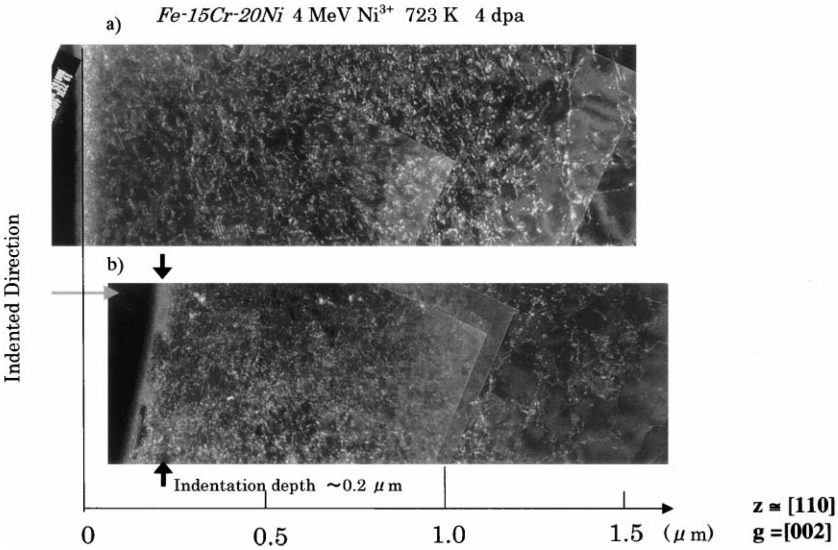


Fig. 2. Cross-sectional TEM image in a single ion-irradiated specimen (4 dpa, 723 K): (a) the region away from the indent; (b) the region beneath the indent.

near $z = [1\,1\,0]$, $g = [0\,0\,2]$. The left side is the irradiated surface. Fig. 2(b) compares a dark field image of the region beneath the indent. As a result of a 9.8 mN (1.0 gf) indentation, Frank loops almost completely disappeared in the region right beneath the indent. When normalized by true indentation depth ($h_c = 307$ nm), which was obtained from an analysis of indentation testing, Frank loops had disappeared in the region from the surface to 2.9 $h_c$. However, in the region from 2.9 to 4.5 $h_c$, a small fraction of Frank loops appeared to have survived the indentation, as shown in Fig. 3, in which a dark field image was taken from one of $\langle 1\,1\,1 \rangle$ satellite spots corresponding to a stacking fault. Detailed size distribution analysis revealed that only Frank loops with diameters in the range 20–25 nm were remaining there, while the original size distributed from <5 to 35 nm with a broad peak at around 15 nm. The fact that Frank loops smaller than 20 nm completely disappeared in spite of the fact that slightly larger loops were remaining leads to an interpretation that they had been swept away by moving dislocations through an elastic interaction. Since small Frank loops are reportedly fair to strong deformation barrier, their complete annihilation through an elastic interaction with sliding dislocations may potentially cause plastic instability in low-temperature irradiated austenitics. Larger Frank loops would not cause such elastic instability, because they appeared to be reacting with moving dislocations by which significant hardness reduction should not occur.

Fig. 4 shows the cavity and dislocation micro-structure in the region right beneath the 9.8 mN indentation in a dual ion-irradiated specimen (873 K, 25 dpa, 10 appm He/dpa at depth of 550 nm). Many voids, which have a mean diameter of about 32 nm, were observed in a depth range 0.02–1.4 μm. The additional irradiation-produced micro-structural features were network dislocations and a small amount of Frank and perfect loops. Therefore, the major contributors to the hardening are likely to be voids and network dislocations in this case. Figs. 4(a)–(c) show the enlarged images of cavity micro-structures of parts of Fig. 4. These cavities were observed to have been shear-deformed along typical mass-flow directions during indentation deformation within a range of 2.7 $h_c$ ($h_c = 349$ nm) from the indentation center. Particularly large cavity deformation occurred in a region where strong compression had been applied by one of the indenter faces. Any Orowan loops or evidence of strong dislocation pinning at the cavities were not observed. This observation suggests that the cavities are readily sheared by sliding dislocations.

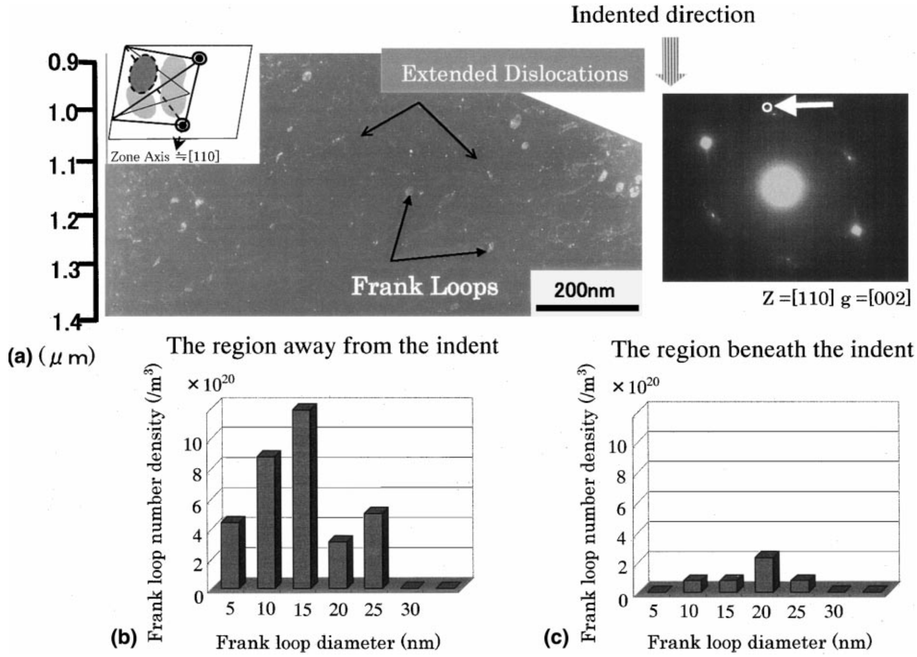


Fig. 3. Image and size distribution of remaining Frank loops in the indented microstructure: (a) dark field image of remaining Frank loops in the region beneath the indent; (b) the region away from the indentation-induced deformation; (c) the region beneath the indent.

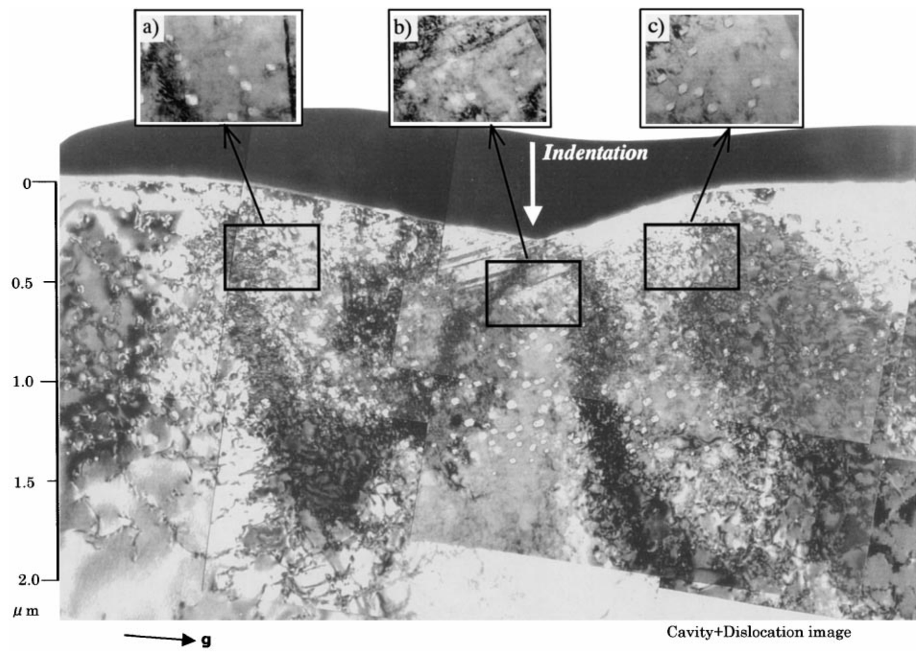


Fig. 4. The image of shear-deformed cavity micro-structure in a dual ion-irradiated specimen: (a)–(c) enlarged images.

According to the expression of Orowan's dispersed barrier equation, the change in shear strength due to planer defects can be written as

$$\Delta\tau = \alpha\ Gb(Nd)^{-0.5},$$

where $G$ is the shear modules, $b$ the Burgers vector magnitude, and $\alpha$ is a measure of barrier strength [9]. $(Nd)^{-0.5}$ is the average barrier spacing, where $N$ and $d$ are the obstacle's number density and average diameter, respectively. Taking $\alpha = 1$ [10,11], the relationships of $\Delta\sigma_y \approx 3.1\Delta\tau$ [12] and $\Delta H \approx 3\Delta\sigma_y$ [13] give approximately 1.18 GPa of $\Delta H$ by the dual-beam irradiation, in spite of the measured $\Delta H$ of 0.35 GPa. This calculation supports that the cavities produced by ion irradiation in model austenitic alloy do not possess strong barrier strength, and suggest that the reported $\alpha$ for voids as high as 1 in neutron-irradiated austenitic stainless steels are associated with radiation-induced solute segregation and/or cavity–precipitate association.

## 4. Summary

The single-beam irradiation at 723 K resulted in a large hardening of austenitic model ternary, mainly due to production of Frank dislocation loops. A very significant reduction in the Frank loop density occurred in the habitation region of moving dislocations during micro-indentation. The complete annihilation of Frank loops smaller than 20 nm in diameter suggested an elastic interaction between Frank loops and sliding dislocations and potential plastic instability of irradiated austenitic alloys which consist mostly of small Frank loops.

The cavity and network dislocation micro-structure produced by the dual-beam irradiation caused a moderate hardening. A comparison of the dispersed barrier model calculation and the measured hardening lead to a substantially weaker barrier strength of cavities than reported for neutron-irradiated austenitics, along with the observation of large shear deformation of, no Orowan loops at and no significant dislocation pinning at cavities.

## Acknowledgements

The authors would like to acknowledge the contributions of Dr H. Shibata and Messrs. M. Narui and T. Omata to the experimental work at the HIT Facility, University of Tokyo.

## References

[1] A. Kohyama, M.L. Grossbeck, G. Piatti, J. Nucl. Mater. 191–194 (1992) 37.
[2] S.J. Zinkle, W.C. Oliver, J. Nucl. Mater. 141–143 (1986) 548.
[3] P.M. Rice, R.E. Stoller, B.N. Lucus, W.C. Oliver, Proc. Mater. Res. Soc. Symp. 373 (1995) 205.
[4] Y. Katoh, H. Tanigawa, T. Muroga, T. Iwai, A. Kohyama, J. Nucl. Mater. 271&272 (1999) 115.
[5] M. Ando, Y. Katoh, H. Tanigawa, A. Kohyama, J. Nucl. Mater. 271&272 (1999) 111.
[6] Y. Katoh, Y. Kohno, A. Kohyama, J. Nucl. Mater. 205 (1993) 354.
[7] Y. Kohno, K. Asano, A. Kohyama, K. Hasegawa, N. Igata, J. Nucl. Mater. 141–143 (1986) 794.
[8] J.P. Biersack, L.G. Haggmark, Nucl. Instrum. and Meth. 174 (1980) 257.
[9] J.W. Martin, Micromechanisms in Particle-Hardened Alloys, Cambridge University, Cambridge, 1980.
[10] G.R. Odette, D. Frey, J. Nucl. Mater. 85&86 (1979) 817.
[11] F. Garner, M. Hamilton, N. Panayotou, G. Johnson, J. Nucl. Mater. 103&104 (1981) 803.
[12] U.F. Kocks, Metall. Trans. 1 (1970) 1121.
[13] G.E. Lucas, G.R. Odette, R. Maiti, J.W. Sheckherd, ASTM STP 956, ASTM, Philadelphia, 1987, p. 379.